Virus Research 261 (2019) 1–8

Contents lists available at ScienceDirect

Virus Research

journal homepage: www.elsevier.com/locate/virusres

Annexin A2 associates to feline calicivirus RNA in the replication complexes from infected cells and participates in an efficient viral replication

Juan Carlos Santos-Valencia[1], Clotilde Cancio-Lonches[1], Adrian Trujillo-Uscanga, Beatriz Alvarado-Hernández, Anel Lagunes-Guillén, Ana Lorena Gutiérrez-Escolano*

Departamento de Infectómica y Patogénesis Molecular, Centro de Investigación y de Estudios Avanzados del IPN, Mexico City, Mexico

ARTICLE INFO

Keywords:
Feline calicivirus
Annexin A2
RNA-protein interaction
Viral replication
Replication complexes

ABSTRACT

Cellular proteins have been identified to participate in calicivirus replication in association with viral proteins and/or viral RNAs. By mass spectrometry from pull-down assays, we identified several cellular proteins bound to the feline calicivirus (FCV) genomic RNA; among them the lipid raft-associated scaffold protein Annexin (Anx) A2. AnxA2 colocalizes with FCV NS6/7 protein and with the dsRNA in infected cells; moreover, it was found associated with the viral RNA in the membrane fraction corresponding to the replication complexes (RCs), suggesting its role during FCV replication. AnxA2-knockdown from CrFK cells prior to infection with FCV caused a delay in the cytopathic effect, a strong reduction of viral non-structural proteins and dsRNA production, and a decrease of FCV yield in both cell-associated and supernatant fractions. Taken together, these results indicate that AnxA2 associates to the genomic RNA of FCV and is required for an efficient FCV replication.

1. Introduction

Feline calicivirus (FCV), a member of the *Vesivirus* genus in the *Caliciviridae* family, causes a highly contagious disease in domestic cats, lions and many other feline species (Guo et al., 2018), which is associated with signs of conjunctivitis (Cai et al., 2002), ulcers in the oral cavity, limping syndrome and mild upper respiratory signs; moreover, it has been associated with abortion and chronic stomatitis in cats (Ellis, 1981; Harrison et al., 2007; Knowles et al., 1989; Thiel and Konig, 1999). FCV has been extensively used as a model for studying calicivirus replication and biology since it replicates efficiently in feline cell culture (Sosnovtsev and Green, 1995; Sosnovtsev et al., 2003).

The members of the *Caliciviridae* family comprise non-enveloped viruses with positive-stranded RNA genomes (Carter, 1990; Simmonds et al., 2008). Particularly, FCV contain three open reading frames (ORFs): ORF1 encodes a polyprotein, which is cleaved by the viral cysteine proteinase (NS6/7) into 6-nonstructural proteins (NS1-NS6/7); ORF2 encodes a precursor protein that is processed by the same viral proteinase producing the major capsid protein VP1 and leader of the capsid protein (LC) (Neill et al., 1991). ORF3 encodes for the minor capsid protein VP2 (Herbert et al., 1997; Neill et al., 1991; Sosnovtsev et al., 1998). All these proteins are present in the enzymatically active replication complexes (RCs) isolated from FCV infected cells (Bailey et al., 2010).

As in many other RNA viruses, besides viral components, cellular proteins have essential roles that contribute to calicivirus life cycle. A number of well-known cellular RNA binding proteins have been identified to bind the 5′ and 3′ ends of the FCV, murine norovirus (MNV), and Norwalk virus (NV) (Gutierrez-Escolano et al., 2000, 2003; Karakasiliotis et al., 2006, 2010; Vashist et al., 2012); among them, the polypyrimidine tract binding (PTB) protein, nucleolin, the poly C binding protein (PCBP) 2, and the heterogeneous nuclear ribonucleoprotein A1 (hnRNP A1) play roles in viral translation control and genome circularization (Cancio-Lonches et al., 2011; Gutierrez-Escolano, 2014; Hernandez et al., 2016; Karakasiliotis et al., 2010; Vashist et al., 2015). Another cellular protein that interacts with viral components is Annexin A2 (AnxA2), a pleiotropic protein involved in essential biological processes such as endocytosis (Rentero et al., 2018), exocytosis, membrane trafficking (Babiychuk and Draeger, 2000; Stewart et al., 2018), cell division and proliferation (Chiang et al., 1999) and phospholipid vesicles aggregation(Stewart et al., 2018). AnxA2 interacts with the FCV LC, a viral protein that has been associated with the cytopathic effect during infection (Abente et al., 2013); however, the specific role of AnxA2 in FCV replication has not been

* Corresponding author at: Departamento de Infectómica y Patogénesis Molecular, Centro de Investigación y de Estudios Avanzados del IPN, Av. IPN 2508. Col. San Pedro Zacatenco, México City, C.P. 07360, Mexico.
E-mail address: alonso@cinvestav.mx (A.L. Gutiérrez-Escolano).
[1] These authors contributed equally to this work.

https://doi.org/10.1016/j.virusres.2018.12.003
Received 22 June 2018; Received in revised form 7 December 2018; Accepted 8 December 2018
Available online 10 December 2018
0168-1702/

determined yet.

AnxA2 is a 39 kDa (36 kDa by SDS-PAGE) protein, member of the annexin family, which is highly expressed in the majority of cells and tissues and bind to numerous ligands (Grindheim et al., 2017). AnxA2 resides soluble in the cytoplasm, or associated with the actin cytoskeleton, the extra or intracellular sides of the plasma membrane, and in some cases in a small fraction from the nucleus (Kazami et al., 2015). This various cellular locations reflect its multiple functions, including vesicle budding, fusion, internalization, late endosomal biogenesis, and membrane repair (Babiychuk and Draeger, 2000; Gerke and Moss, 2002; Madureira et al., 2011; Morel and Gruenberg, 2007; Moss and Morgan, 2004; Rescher and Gerke, 2004; Sarafian et al., 1991). All this multifunctionality is subjected to ligand binding and post-translational modifications, especially phosphorylation (Grindheim et al., 2017). AnxA2 has also been implicated in the RNA metabolism, particularly in the subcellular localization and translational regulation of messenger RNAs (mRNAs), because of its association with the 3′ UTR of some cellular RNAs including its own (Filipenko et al., 2004; Hollas et al., 2006; Mickleburgh et al., 2005). Furthermore, AnxA2 has been identified as a host factor regulating several key processes of many viruses, from entry to assembly and morphogenesis (Gonzalez-Reyes et al., 2009; Li et al., 2014a; Ma et al., 2017; Sheng et al., 2015; Yang et al., 2011; Zhang et al., 2010). Particularly during HCV replication, AnxA2 recruits NS proteins and enriches them in lipid rafts to facilitate the formation of the viral RCs and contributes to the formation of infectious HCV particles (Backes et al., 2010; Saxena et al., 2012). In the present study, we identified that AnxA2 associates with the FCV RNA, and showed that AnxA2 plays a role in FCV replication.

2. Materials and methods

2.1. RNA pull down assay

To identify cell proteins that interact with the stem loop structure present in the 3′UTR from FCV RNA, a biotinylated-RNA was obtained by *in vitro* transcription as previously described (Hernandez et al., 2016), in the presence of biotinylated-UTP. Briefly, an amplicon corresponding to the last 36 nt from the FCV genomic RNA without the poly (A) tail was obtained by polymerase chain reaction (PCR) from FCV-infected CrFK cells cDNA using a sense primer that contained the bacteriophage T7 promoter sequence, FW 5´-TAATACGACTCACTATAGGGTAATACGACTCACTATAGGGCCCTTTGGGCTGCCG-3′ and RV 5´−CCCTGGGGTTAGGCGCAAATGCG-3′) (Hernandez et al., 2016). Four mg/ml of total FCV infected cell extracts treated with micrococcal nuclease, following the manufacture's instructions (New England Biolabs), were pre-absorbed with 50 µl of streptavidin agarose beads in a final volume of 1.5 ml of RIPA buffer (25 mM Tris−HCl [pH7.4], 150 mM NaCl, 1% NP40, 0.01% SDS, 0.5% sodium deoxycholate) containing protease inhibitors (Roche) for 3 h gently shaking at 4 °C. Pre-absorbed extracts were recovered by centrifugation at 2500 rpm for 5 min, at 4 °C; then, 30 µl of the streptavidin agarose beads were pre-incubated with tRNA at a final concentration of 0.1 µg/µl followed by the addition of 14 µg of the biotinylated–RNA from the FCV 3′ UTR for 4 h, at 4 °C. The streptavidin agarose beads coupled to the biotinylated-RNA were interacted with the pre-absorbed total cell extract for 2 h at 4 °C. Finally, the ribonucleoprotein complexes were pulled down by centrifugation at 2500 rpm for 5 min, at 4 °C, washed 5 times with RIPA buffer for 5 min at 4 °C, resuspended in 10 µl of Laemmli buffer and boiled for 10 min. The samples were separated by SDS-PAGE for 20 min at 80 V. The gel was washed 3 times for 5 min with milliQ water. Proteins were stained with 50 ml Coomassie blue (blue R-250, Bio-Rad) for 30 min at RT; the bands were cut and analyzed by MALDI-TOF (MS/MS) in the Proteomics Lab Facility at CINVESTAV Irapuato, Mexico. The MS/MS data were analyzed using Proteome Discoverer 1.4 software, set up to search the *Felis catus* NCBI database.

2.2. Cells and virus infection

The CrFK culture cells and the FCV (strain F9) were obtained from the American Type Culture Collection (ATCC) (Rockville, MD). Cells were grown in Eagle's minimal essential medium with Earle's balanced salt solution and 2 mM L-glutamine that was modified by the ATCC to contain 1.0 mM sodium pyruvate, 0.1 mM nonessential amino acids, 1.5 g/l sodium bicarbonate. The medium was supplemented with 10% bovine fetal serum, 5000 U of penicillin and 5 µg/ml of streptomycin. Cells were grown in a 5% CO2 incubator at 37 °C. The cytopathic effect (CPE) induced by FCV infection was monitored at 5 hpi by evaluating cell morphology using a brightfield microscope. Virus titers in the supernatants and cell-associated fractions from cells treated with NT- and AnxA2-siRNAs were determined by plaque assay as previously described (Escobar-Herrera et al., 2006). For total cell extracts, CrFK cells were washed twice with phosphate buffered saline (PBS) (0.137 M NaCl, 2.7 mM KCl, 1.4 mM KH_2PO_4, 0.01 M Na_2HPO_4) an resuspended in 5 cell volumes of RIPA buffer in the presence of protease inhibitors (Roche) for 10 min at 4 °C. Cells were centrifuged at 14,000 rpm for 15 min and the supernatant was quantified using the BCA protein Assay kit (Pierce).

2.3. Electrophoretic mobility shift assay (EMSA)

Total cell extracts (20 µg of protein) from CrFK cells were obtained an quantified as described above, and pre-incubated with the same amount of tRNA in a buffer containing 10 mM HEPES (pH 7.4), 0.1 mM EDTA, 0.2 mM dithiothreitol (DTT), 8 mM $MgCl_2$, 4 mM spermidine, 3 mM ATP, 2 mM GTP, and 10% (vol/vol) glycerol for 30 min at 4 °C. Rabbit anti-goat IgG-HRP (sc-2678, Santa Cruz Biotechnology), used as a non-related antibody, or the polyclonal anti-AnxA2 antibody (sc-9061, Santa Cruz Biotechnology) were added to the reaction mixture in a final volume of 15 µl, for 15 min at 4 °C before or after the addition of 4×10^5 cpm of [α-^{32}P] UTP labeled RNA corresponding to the stem loop structure present in the last 36 nt from the FCV 3′UTR (without the poly (A) tail as indicated. The reaction was incubated for 15 min at 4 °C followed by RNase treatment (20 U of RNase A and 20 µg of RNase T1) for an additional 15 min at room temperature (RT). The RNA-protein complexes were analyzed in a 10% native gel as described before (Gutierrez-Escolano et al., 2003).

2.4. Immunofluorescence assay

CrFK cells were grown overnight on glass coverslips and infected with FCV at an multiplicity of infection (M.O.I.) of 5 at the indicated times. The cells were treated with cytoskeleton buffer (CB) [10 mM MES (SigmaM-8250), 150 mM NaCl, 5 mM $MgCl_2$, and 5 mM glucose] for 5 min and permeabilized in 4% paraformaldehyde solution containing Triton X-100 0.2% for an additional 5 min at RT. The samples were washed three times for 5 min with PBS and incubated with the anti-AnxA2 antibody at 4 °C overnight. The samples were washed three times for 5 min with cold PBS, incubated with the corresponding secondary antibody (Invitrogen) for 1 h at RT, washed three times with PBS, and incubated with an anti-NS6/7, (kindly donated by Ian Goodfellow, University of Cambridge, UK), or anti-dsRNA antibodies (MAb J2 anti-dsRNA, kindly donated by Mariano Garcia Blanco/Bradrick lab from University of Texas Medical Branch) over night at 4 °C. The samples were washed three times with PBS, incubated with the corresponding secondary antibody (Invitrogen) for 1 h at RT, washed three times with PBS, and incubated with 1 µg/µl of 4′,6-diamidino-2-phenylindole dihydrochloride (DAPI) for 2 min. The samples were washed six times with PBS and three times with filtered distilled water. Finally, the samples were mounted with Vecta-Shield (Vector Laboratories A.C.) and analyzed using a Zeiss LSM-700 confocal microscope. Colocalization rates were calculated by Pearson´s coefficient.

2.5. Western blot analysis

Mock and infected CrFK cells were washed with PBS, lysed in NP-40 cell lysis buffer (50 mM Tris − HCl pH7.4, 150 mM NaCl and 1% NP-40), then, Laemmli sample buffer was added and boiled for 10 min. Approximately twenty µg of protein extract were analyzed by SDS-PAGE and transferred to nitrocellulose membranes. The membranes were blocked with 10% skimmed milk for 2 h and incubated overnight at 4 °C with the following antibodies: monoclonal (sc-48397, Santa Cruz Biotechnology) or polyclonal anti-AnxA2, polyclonal anti-Protein Disulfide Isomerase (PDI) (sc-74551, Santa Cruz Biotechnology), anti-actin (kindly donated by Manuel Hernández, Cinvestav, México), and anti-N6/7. The blots were washed extensively with 0.05% Tris-buffered saline (TBS)-Tween and incubated for 2 h with the appropriate secondary antibodies and developed using the SuperSignal west femto maximum sensitivity substrate kit (Thermo scientific). Protein quantification was achieved by the band intensities in the scanned images using ImageJ software (http://rsb.info.nih.gov/ij) and expressed as arbitrary units.

2.6. Viral RNA amplification from AnxA2 immunoprecipitated fractions from the replication complexes

Membrane fractions corresponding to FCV RCs were obtained from infected CrFK cells as described previously (Green et al., 2002). Briefly, 2×10^7 CrFK cells were mock infected or infected with FCV at an MOI of 5 as described above. After 5 h cells were pelleted by centrifugation at 1500 rpm for 5 min at 4 °C. The cell pellet was resuspended in 250 µl ml of cold TN buffer (10 mM Tris [pH 7.8], 10 mM NaCl) and incubated for 15 min at 4 °C. After 15 min on ice, the cells were lysed with 60 strokes in a cold 2-ml glass Dounce homogenizer. The lysate was centrifuged for 5 min at 3000 rpm for 5 min, at 4 °C to remove nuclei and unlysed cells. The supernatant was centrifuged for 20 min at 14,000 rpm for 20 min, at 4 °C. The resulting pellet was resuspended in 120 µl of TN buffer with 15% glycerol and stored at −70 °C. These resuspended fractions correspond to FCV RCs or mock RCs. The amount of protein in each fraction was determined with the Coomassie Plus Protein Assay Reagent (Pierce). Immunoprecipitation of AnxA2 from the RCs was carried out using the monoclonal anti-AnxA2 antibody. An anti-GFP antibody (SC-9996, Santa Cruz Biotechnology) was used as a negative control. The viral RNA coimmunoprecipitated in the RC was subjected to reverse transcription and polymerase chain reaction (RT-PCR) using MLV (Invitrogen) and viral-RNA-specific primers (FWD 5′ TTAGCTTATGTAGGACCAGGCACCAAGTTCCAC and REV 5′TTTAAGC TTAACTTCGAACACATCACAGTGTAGGGC) to produce a 2073-bp product corresponding to the NS6/7 region from the FCV genome.

2.7. siRNA-mediated knockdown of AnxA2

Protein database searches were performed with the National Center for Biotechnology Information services (https://www.ncbi.nlm.nih.gov/). Based on the obtained full-length feline AnxA2 RNA sequences, the comparison and alignment of the AnxA2 translation products were performed using the ClustalW multiple-alignment program. Two different siRNAs corresponding to coding region nucleotides 148–(siAnx2-1: 5′ − CCGCAGCAAUGAACAGAGAUU-3′) and 274-(siAnx2-2: 5′- AAC ACCUGCUCAGUAUGAUUU -3′) were designed using the Custom RNAi Design Tool from The RNAi WEB (Integrated DNA Technologies, Inc.). For siRNA-mediated knockdown of AnxA2 expression, transfections were carried out according to the protocol recommended by the manufacturer (siPORT amine transfection agent; Applied Biosystems, Mexico). Briefly, CrFK cells were plated in a 6-well plate to reach 60% confluence. After 24 h, 5 µl of siPORT and 200 nM siRNAs for AnxA2 were mixed separately with 100 µl Opti-MEM, for 10 min at RT. The two mixtures were combined, allowed to incubate at RT for 10 min, and diluted to 1 ml with 800 µl Opti-MEM. The mixture was added directly to the cells, and transfection with the siRNAs was carried out at 37 °C for 8 h, followed by the addition of 1 ml of growth medium and an additional incubation up to 72 h. CrFK cells were also treated with a non-targeting (NT)-siRNA (SC-37007, Santa Cruz Biotechnology) as a control. After 72 h transfection, cells were infected with FCV at an MOI of 5 and harvested at 5 h post-infection. The levels of the AnxA2, actin, and NS6/7 proteins were determined by Western blotting. The viability of NT-siRNA and-AnxA2-siRNA-treated cells was determined at 72 h using a CellTiter 96 assay (Promega), following the manufacturer's instructions.

3. Results

3.1. AnxA2 is associated with the FCV 3′-UTR RNA in vitro and in infected cells

It is well known that viruses hijack cellular components that participate in different steps of its replication. Some cellular proteins have been identified because they are modulated or relocated during viral infections, some others, because of its association with viral proteins or with the viral RNAs. To identify proteins that interact with the 3′UTR from the FCV RNA, *in vitro* transcribed biotinylated RNA from the FCV 3′ UTR (Fig. 1A), coupled or not with streptavidin agarose beads was interacted with total cell extracts, and the ribonucleoprotein complexes were pulled down, separated by SDS-PAGE, and analyzed by mass spectrometry (Maldi-Tof) (Fig. 1B). Sixteen proteins were identified associated with the biotinylated RNA that were absent in the controls

A

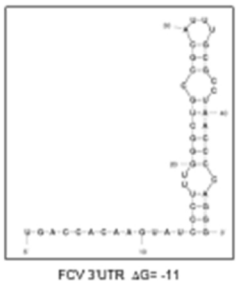

B

Protein ID	Accession no.	Mass (kDa)	Score (%)
PCCB	XP_011284436	58.2	97.5
PCCA	XP_019684638	77.3	86.6
PC	XP_019668279	129.6	16.5
TUBA1C	XP_011282203	49.9	17.5
GAPDH	NP_001009307	35.8	15.0
ANXA2	XP_003987117	38.6	32.6
YBX1	XP_023114340	21.7	42.1
ACTG1	XP_023100072	41.8	20.9
ALB	NP_001009961	66.8	33.4
TUBA1A	XP_023112782	48.6	33.3
YBX2	XP_023100501	40.0	29.6
YBX3	XP_023112546	40.9	36.8
EEF1A1	NP_001009326	51.0	3.83
TUBB2A	XP_023109488	48.9	22.4
PKM	XP_019690033	57.9	23.8
SSB/La	XP_011285625	41.0	46.7

Fig. 1. Proteins bound to the 3′UTR rom the FCV identified by mass spectrometry.
A) Predicted secondary structure of the FCV 3′UTR using MFold2 software (http://mfold.rna.albany.edu/?q_mfold/RNA_Folding_Form2.3). B). Host factors from CrFK cell extracts that interacted with the 3′ UTR of the feline calicivirus genome. *In vitro* transcribed biotinylated RNA from the FCV 3′ UTR coupled or not with streptavidin agarose beads was interacted with total cell extracts. The ribonucleoprotein complexes were pulled down and separated by SDS-PAGE, stained by Coomassie blue and analyzed by mass spectrometry (Maldi-Tof). The proteins were identified from three independent experiments.

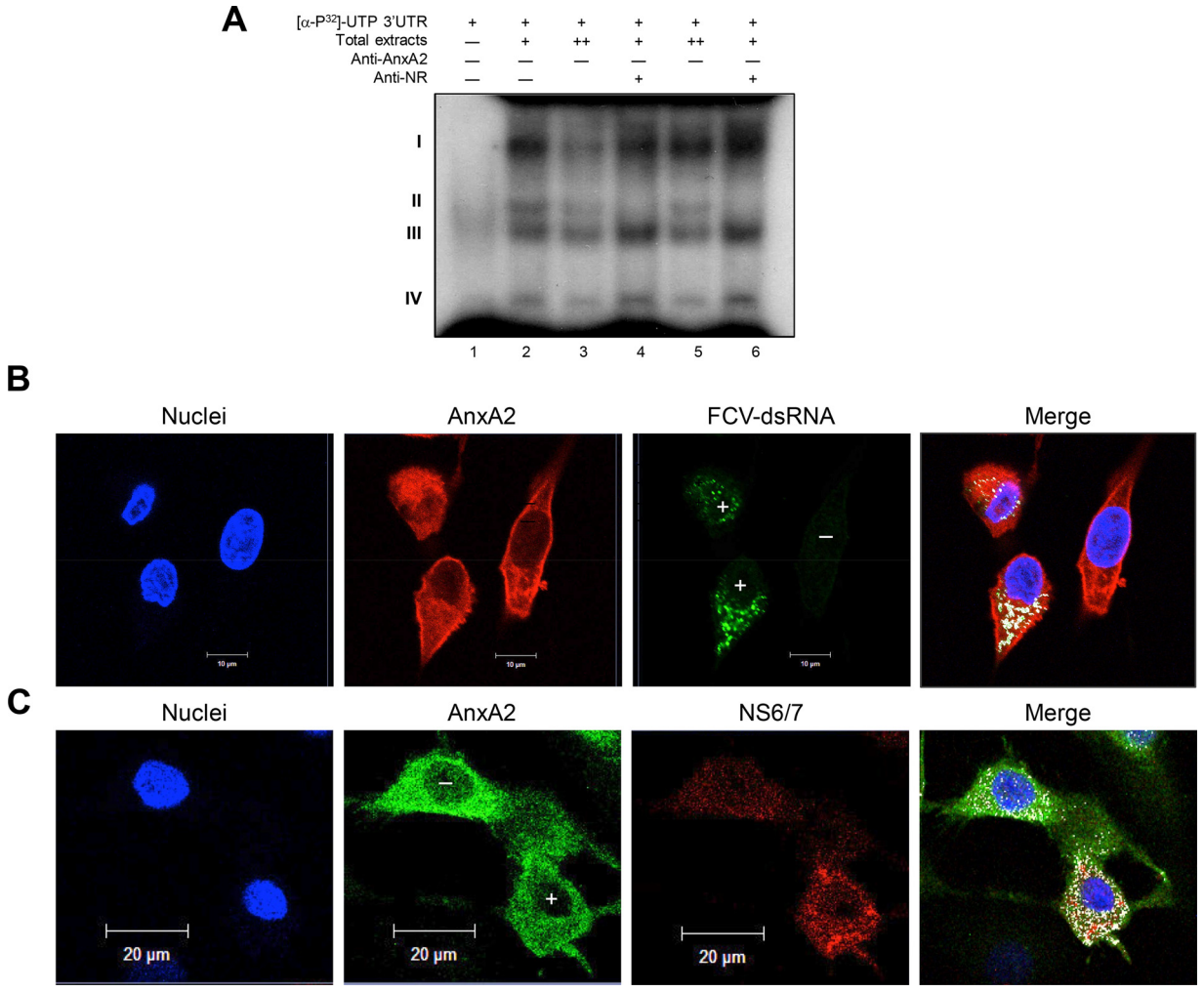

Fig. 2. AnxA2 is *in vitro* associated with the FCV 3′UTR RNA and with the viral NS6/7 protein during infection. A) Mobility shift assay of the [α-^{32}P]-UTP-labeled FCV 3′UTR RNA incubated with the CrFK protein cell extract (lane 2–4) in the absence (lane 2) or the presence of human anti-AnxA2 (lanes 3 and 5) or anti-NR (non-related) (lanes 4 and 6) antibodies. RNA was incubated with the protein cell extract prior (lanes 3 and 4) or after (lanes 5 and 6) the addition of antibodies. Lane 1, free RNA. The position of the formed complexes (I–IV) is shown. Monolayers of CrFK cells were infected with FCV at an MOI of 5 for 5 hpi fixed and stained for B) AnxA2 (polyclonal anti-AnxA2, red) and dsRNA (monoclonal anti-dsRNA, green) and C) AnxA2 (polyclonal anti-AnxA2, green) and NS6/7 (polyclonal anti-NS6/7, red). Non-infected (-) and infected cells (+) are indicated. DAPI was used for nuclear (blue) staining. The cells were examined in a Zeiss LSM700 laser confocal microscope. Images correspond to a z-stack of 15 slices. Scale bars of 10 µm are shown. Pearson´s coefficient was 0.65 ± 0.17 for AnxA2 and dsRNA and 0.56 ± 0.14 for AnxA2 and NS6/7.

without the biotinylated RNA; among them, proteins previously reported to interact with the human and murine norovirus 3′ UTR from the RNA genome such as the SSB/La autoantigen or La protein, the eukaryotic elongation factor (eEF1) -□1, and the glyceraldehyde 3-phosphate-dehydrogenase (GAPDH) (Gutierrez-Escolano et al., 2003; Vashist et al., 2012). Moreover, we also identify other well-characterized host factors implicated in mitochondria metabolism, such as propionyl-CoA carboxylases and the pyruvate carboxylase, and proteins from and associated with the cytoskeleton such as actin, tubulin, and the lipid raft-associated scaffold protein AnxA2 (Fig. 1B).

3.2. AnxA2 is associated with the FCV 3′-UTR RNA in vitro and in infected cells

To corroborate that AnxA2 was present in the ribonucleoprotein (RNP) complex formed with the FCV 3′ UTR, two different assays were done. First, an EMSA was performed in the presence of an anti-AnxA2 antibody (Fig. 2A). Four-well defined complexes named as I, II, III, and IV were observed when the FCV 3′ UTR interacted with total CrFK protein extracts (Fig. 2A, lane 2). When the anti-AnxA2 antibody was incubated with CrFK protein extracts prior to the addition of the labeled RNA, the formation of all complexes was reduced (Fig. 2A, lane 3), suggesting the presence of AnxA2 in these complexes. However, the same amount of an unrelated antibody (anti-NR) altered complex II formation but did not modify complexes I, III and IV (Fig. 2A, lane 4), indicating that AnxA2 is present in these three specific complexes. Moreover, when the labeled RNA was incubated with the cell extracts prior the addition of the anti-AnxA2 and the non-related (NR) antibodies, the formation of complexes I, III and IV was not modified (Fig. 2A, lanes 5 and 6 respectively), indicating that AnxA2 interact in the same region with both the RNA and the anti-AnxA2 antibody. Complex II was considered unspecific since it is reduced in the presence of anti-AnxA2 and NR antibodies in both conditions. The specificity of the anti-AnxA2 but not anti-IgG-HRP antibody to detect AnxA2 in the cell extracts is shown in Supplementary Fig. 2. All this results suggest that AnxA2 is associated with the 3′UTR RNA from the FCV.

The association between AnxA2 and FCV RNA in infected cells was also determined by immunofluorescence assays using anti-dsRNA and anti-AnxA2 antibodies (Fig. 2B). The subcellular distribution of AnxA2 (red) was clearly observed in the cellular membrane as well as in the

cytosol of both mock-infected (-) and infected (+) cells at five hours post infection (hpi). Moreover, a co-localization between AnxA2 and the FCV-dsRNA (green) was observed (white) (Fig. 2B: Merge). A co-localization rate was 0.65 ± 0.17. Taken together, these results strongly suggest that AnxA2 is associated with FCV RNA and *in vitro* and in infected cells.

3.3. AnxA2 is present in FCV RCs where it is associated with the viral RNA

Since most of the viral RNA was associated with AnxA2, it was possible that this protein was present in the RCs. To further determine if AnxA2 was present in the RC, its association with other component of this compartment, the protease-polymerase NS6/7 was investigated. The subcellular distribution of AnxA2 (green) was clearly observed in the cellular membrane as well as in the cytosol of both mock-infected (-) and infected (+) cells at five hpi. Although no changes were observed in the expression (Supplementary Fig. S1) or localization of AnxA2 during FCV infection, a co-localization between AnxA2 and FCV NS6/7 (red) staining was observed in the perinuclear area (Fig. 2C). A co-localization rate was 0.56 ± 0.14. The Co-localization of AnxA2 with two of the main components of RCs, the dsRNA and the protease-polymerase NS6/7 strongly suggest that this cellular protein is present in the RCs.

To confirm that AnxA2 is present in the RCs, CrFK cells were infected with FCV at an M.O.I. of 5, at 5 hpi, RCs were isolated, and the presence of AnxA2, NS6/7, and PDI, a protein resident of the endoplasmic reticulum, was analyzed by western blotting (Fig. 3). The presence of PDI and AnxA2 was observed in the RC membrane fractions from infected cells as well as in the corresponding membranous fractions from the mock infected cells (Fig. 3A). However, a 3 fold increased amount of AnxA2 was found in the RC membrane fractions from infected cells in comparison to the corresponding membranous fractions from mock-infected cells, indicating that this protein is recruited in the RCs isolated from cells infected with FCV (Fig. 3A and B).

To further determine if AnxA2 was associated with the FCV RNA in infected cells, RCs membranous fractions were isolated from infected cells, as well as the corresponding membrane fractions from mock-infected cells, and subjected to immunoprecipitation assays using anti-AnxA2 and anti-GFP (non-related) antibodies (Fig. 3C). While AnxA2 was not detected when the immunoprecipitation was carried out using a non-related antibody (Fig. 3C upper panel, lanes 2 and 3) it was clearly immunoprecipitated by the anti-AnxA2 antibody (Fig. 3B, upper panel, lanes 4 and 5). To determine the association of viral RNA and the AnxA2 immunoprecipitated from the RCs, the RNA sequence corresponding to the NS6/7 coding region was amplified by RT-PCR. This amplicon was only amplified in the fraction immunoprecipitated by AnxA2 from infected cells (Fig. 3B lower panel, lane 4) but not in the fractions from mock-infected cells or treated with the non-related antibody (Fig. 3C lower panel, lanes 5, 2, and 3) respectively. Taken together, these results indicate that AnxA2 is present in the RCs from FCV infected cells and associated with the viral RNA

3.4. Inhibition of AnxA2 expression results in the reduction of viral protein synthesis and FCV replication

To determine if AnxA2 plays a role during FCV infection its expression was knocked down by using specific siRNAs and the production of the viral non-structural proteins, and dsRNA was analyzed by western blotting and confocal microscopy (Fig. 4). Two siRNAs specifically directed against feline AnxA2 (see materials and methods) were transfected into CrFK cells for 72 h and then, cells were infected with FCV at an M.O.I. of 5, at 5 hpi. The first observation was that AnxA2 knockdown cells displayed a delayed cytopathic effect compared to the non-targeting (NT) siRNA-treated cells (Fig. 4A). Moreover, cell transfection with the AnxA2-siRNA caused the reduction of AnxA2 expression up to 98% (Fig. 4B and C), that resulted in a 96% reduction of NS6/7 levels, compared with the levels from cells transfected with the NT-siRNA (Fig. 4B and C). Cell viability was unaffected by the siRNA treatment (data not shown). The reduction in the expression of NS6/7 as a result of the siRNA-mediated knockdown of AnxA2 levels, suggests that AnxA2 is important for FCV replication. To further support this hypothesis, the dsRNA levels of AnxA2 knockdown cells were investigated. A reduction of 3.4 times in the dsRNA levels was detected in AnxA2 knockdown cells, were red staining was significantly reduced (Fig. 4D lower panel, E, and F), in comparison with the non-transfected cells observed in the same panel, that show similar red staining as the

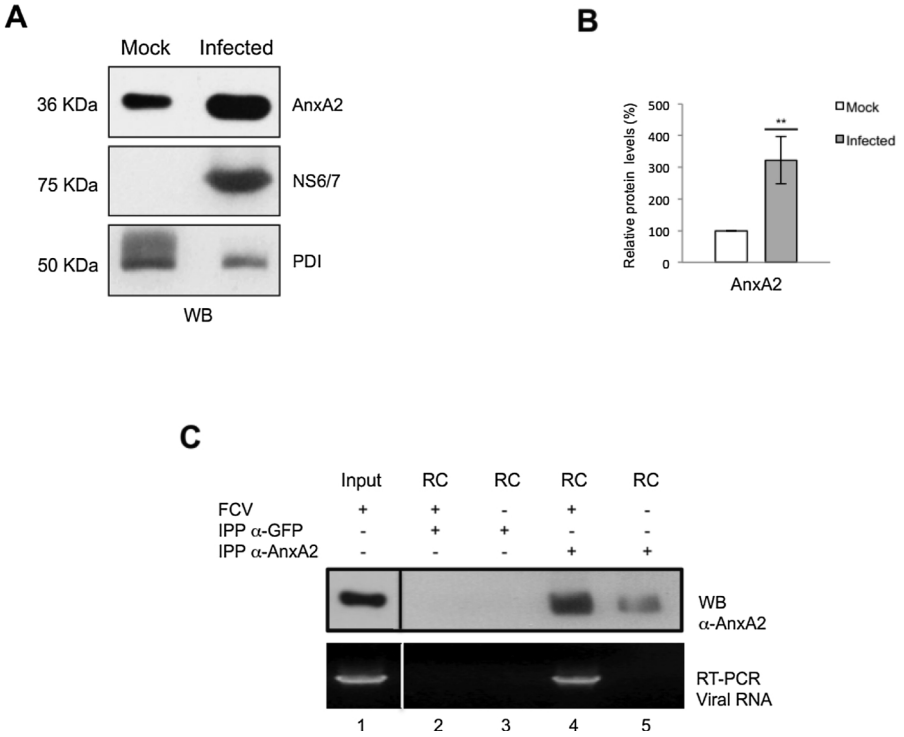

Fig. 3. AnxA2 is associated with the viral RNA in the FCV replication complexes. A) Cell membrane fractions corresponding to replication complexes from infected CrFK cells at an MOI of 5 for 5 h and the corresponding membrane fractions from non-infected cells were isolated and the levels of AnxA2, FCV NS6/7, and PDI used as ER-marker control were evaluated by Western blotting. B) AnxA2 band intensities were quantified by densitometric analysis using ImageJ, and expressed as the percentage of relative intensities in relation to PDI expression level. The statistical tests were performed using the Graph Pad Prism software. $^{**}P \leq 0.0005$ by two-way ANOVA. Error bars represent the standard deviation from three independent experiments. C) Cell membrane fractions corresponding to RC from infected CrFK cells (lanes 2 and 4) and corresponding membranous fractions from mock-infected cells (lanes 3 and 5) were subjected to immunoprecipitation with anti-AnxA2 (lanes 4 and 5) or anti-GFP antibodies (lane 2 and 3). The presence of AnxA2 in the immunoprecipitated fractions was verified by Western blotting (upper panel); the co-immunoprecipitated FCV viral RNA was analyzed by RT-PCR using specific oligonucleotides to amplify the NS6/7 region (lower panel). Input cell extracts are shown in lane 1.

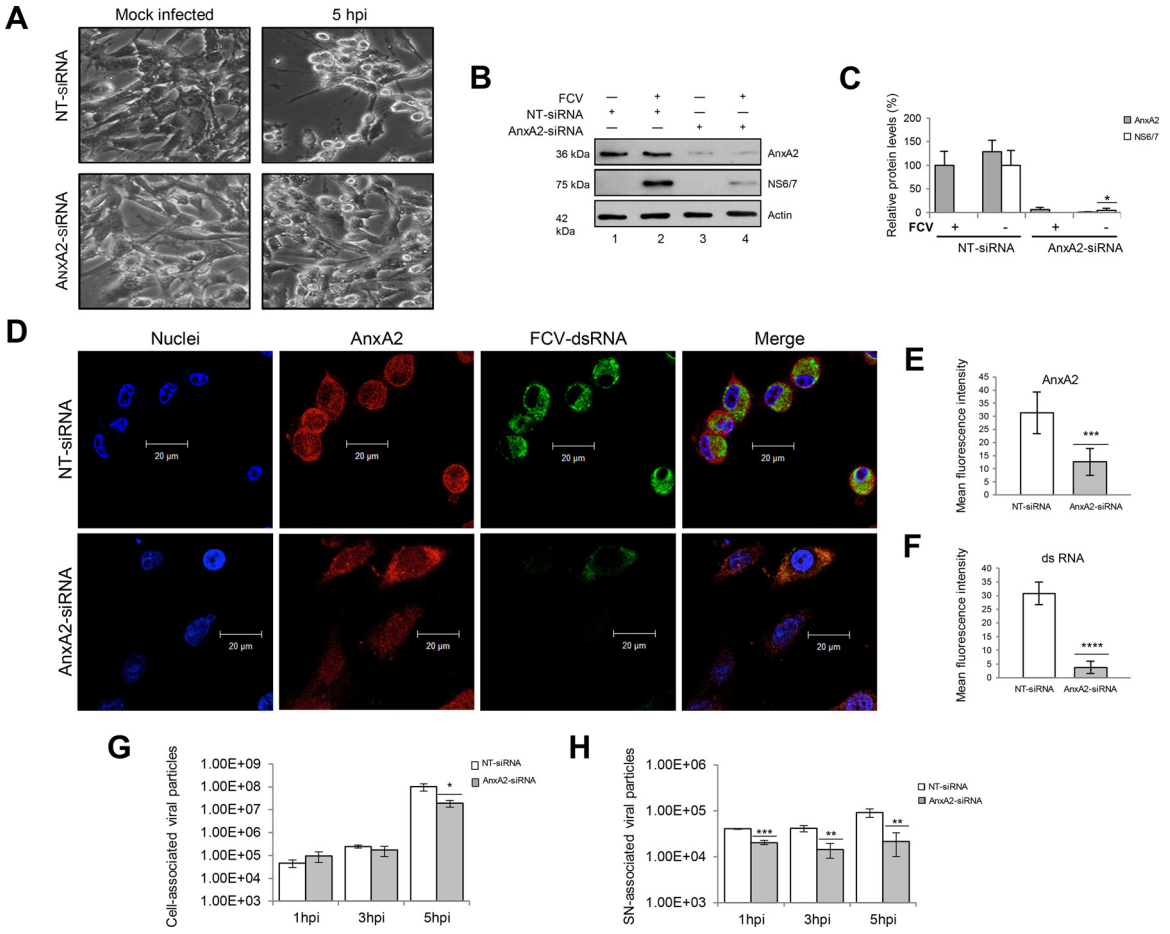

Fig. 4. FCV non-structural protein expression, dsRNA, and virus production are reduced in AnxA2 siRNAs treated cells. Monolayers of CrFK cells were treated with a non-targeting siRNA (NT) or an AnxA2 siRNAs for 72 h and either mock-infected or infected with FCV (MOI 5) for 5 h. A) The cytopathic effect and B) the presence of AnxA2, NS6/7, and actin (load control) proteins in total cell extracts were analyzed by Western blotting using specific antibodies. C) AnxA2 and NS6/7 band intensities were quantified by densitometric analysis using ImageJ software and expressed as the percentage of relative intensities in relation to the actin expression level. Error bars represent the standard deviation from three independent experiments. * $P \leq 0.0001$ by two-way ANOVA analysis. D) The subcellular localization of AnxA2 (red) and dsRNA (green) was determined using a Zeiss LSM700 laser confocal microscope. DAPI was used for nuclear (blue) staining. Merge images are indicated. Scale bars of 20 µm are shown. Images correspond to a z-stack of 15 slices. E) and F) AnxA2 and dsRNA mean fluorescence intensities. The statistical tests were performed using the Graph Pad Prism software. *** $P \leq 0.0005$ **** $P \leq 0.0001$ by two-way ANOVA analysis. Error bars represent the standard deviation from three independent experiments. Levels of cell-associated G) and supernatant-associated H) viral particles from cells infected at an MOI of 1, at 1, 3, and 5 hpi were obtained by plaque assay. Error bars represent the standard deviation from three independent experiments. ***$P \leq 0.0001$ ** $P \leq 0.005$ * $P \leq 0.01$ by Student´s *t*-test.

NT-siRNAs treated cells (Fig. 4D lower panel), and of cells transfected with the NT-siRNA (Fig. 4D upper panel). In agreement with the reduction in the dsRNA and in the viral proteins in AnxA2 knockdown cells, a statistically significant reduction of FCV yield at an MOI of 1, at 5 hpi in the cell-associated and at 1, 3, and 5 hpi in the supernatant-associated fractions was detected (Fig. 4G and H). Moreover, a reduction of approximately 1 log at an MOI of 5, at 5 hpi in both cell-associated and supernatant-associated fractions was also observed (data not shown), indicating that AnxA2 is required for an efficient FCV replication.

4. Discussion

Because of the austerity of their genomes, viruses are strict intracellular parasites that depend on the interaction between the few viral components with the vast amount of cellular factors involved in a wide variety of mechanisms to complete each viral step during its replicative cycle. Information regarding the function of the cellular proteins that interact with viral RNAs and with other viral components during calicivirus replication is still limited (Alhatlani et al., 2015; Cancio-Lonches et al., 2011; Gutierrez-Escolano, 2014; Hernandez et al., 2016; Karakasiliotis et al., 2006; Vashist et al., 2015); however, these interacting cellular proteins represent targets to be explored for the development of antiviral strategies to control and prevent infection.

AnxA2 is a lipid raft-associated scaffold protein that was previously identified as a specific binding partner of the LC protein during FCV infection but whose role in replication remained undetermined (Abente et al., 2013). AnxA2 participates in many of cellular functions, including cell motility, endocytosis, calcium-dependent regulation of exocytosis, DNA synthesis and cell proliferation, membrane trafficking, and cytoskeleton rearrangements (Babiychuk and Draeger, 2000; Gerke and Moss, 2002; Madureira et al., 2011; Morel and Gruenberg, 2007; Rescher and Gerke, 2004; Sarafian et al., 1991). Here we show that AnxA2 was found associated with the 3´UTR from the viral RNA *in vitro* as well as in FCV infected cells by using different approaches.

In addition to its role as a cytoskeletal- and membrane-associated protein, AnxA2 functions as a trans-acting protein binding to cis-acting sequences of eukaryotic as well as viral RNAs, including its own RNA (Aukrust et al., 2017; Hollas et al., 2006; Kwak et al., 2011; Mickleburgh et al., 2005). Several of the AnxA2-binding RNA sequences are found in the 3′ UTRs in accordance with our finding that AnxA2 associates with the FCV 3′ UTR RNA. Besides the ability of AnxA2 to

bind to poly (G) sequences (Filipenko et al., 2004), two conserved AnxA2 binding motifs have been reported; a five nucleotide (nt) AACAG sequence in a stem-loop element of the 3′ UTR from the AnxA2 cognate mRNA (Hollas et al., 2006), and a five nt AUUUA sequence within the 3′ UTR of *c-myc* mRNA (Mickleburgh et al., 2005; Veyrune et al., 1996). Although we have not found these sequences within the FCV 3′ UTR RNA, other sequences, as well as the stem-loop elements present in this region, could also represent AnxA2 binding sites, since it has been widely reported that RNA secondary structures have impact on binding-sites selection of cellular proteins to modulate lifecycle processes (Li et al., 2014b; Liao et al., 2018; Shwetha et al., 2015).

The AnxA2 binding sequence within the 3′ UTR of *c-myc* mRNA, correspond to a localization signal responsible of its association with the cytoskeleton and targeting the c-myc RNA to the perinuclear cytoplasm (Mickleburgh et al., 2005). Post-translational modifications of AnxA2 are linked to its association with perinuclear non-polysomal mRNAs, most probably as a mechanism to sequester subpopulations of mRNAs, and targeting messenger ribonucleoprotein (mRNP) complexes to specific cellular sites, particularly in the perinuclear area (Aukrust et al., 2017). Abente et al., (2013) identified that AnxA2 is a binding partner of the FCV LC protein that was detected on the plasma membrane and along the cytoplasm. In this work, AnxA2 was particularly observed in a perinuclear area that corresponds to the sites were the RC locates (Abente et al., 2013). Thus, it is likely that AnxA2 plays a role targeting the viral RNAs to the RC; yet, direct binding of AnxA2 to the viral RNA and a role in the localization of FCV RNA in this region remains to be determined.

In this work, we demonstrated the *in vitro* association of AnxA2 with the viral RNA, and it´s co-localization with the FCV protease-polymerase NS6/7 protein in the perinuclear area of infected cells, suggesting its presence in the RCs. Moreover, the association of AnxA2 with the FCV RNA in infected cells and its enriched presence in the membrane fraction corresponding to RCs (Fig. 3), clearly demonstrate that AnxA2 is a component of this structure. To this regard, during hepatitis C virus (HCV) replication, AnxA2 recruits NS proteins and enriches them in lipid rafts to facilitate RC formation, and contributing to the morphogenesis of infectious particles (Backes et al., 2010; Saxena et al., 2012; Solbak et al., 2017).

The role of AnxA2 in FCV replication was confirmed in a series of experiments where AnxA2 was knocked down by using specific AnxA2-siRNAs prior to infection with FCV. The strong reduction of AnxA2 correlated with a decrease of viral NS proteins and dsRNA production that was not observed in cells treated with an NT-siRNA. These results, together with the observed delay in the cytopathic effect caused by the infection and the statistical significant inhibition of FCV production in both cell-associated and supernatant-associated fractions, indicate that AnxA2 is required for a FCV efficient replication. Thus, our results are in agreement and expand previous reports where AnxA2 has been identified as a host factor regulating several key processes in many viruses. For example, AnxA2 contributes in the replication of H5N1 avian influenza virus (Ma et al., 2017), in the porcine reproductive and respiratory syndrome virus (PRRSV) replication (Li et al., 2014a), and it is involved in the production of classical swine fever virus infectious particles by binding the viral protein NS5A (Sheng et al., 2015).

The recruitment of AnxA2 in the RCs, as well as its association with the viral RNA, suggest that it is involved in the regulation of RNA and/or protein synthesis, in concordance with the reduction of viral protein synthesis and dsRNA, as a result of AnxA2 knockdown (Fig. 4B and C). Moreover, the reduction of virus yield observed in both, cell-associated and supernatant fractions in AnxA2 knockdown cells could also be related to a deficient viral translation and/or RNA replication. On the other hand, these reduced viral yields could also suggest that AnxA2 function as a scaffold protein for viral assembly, as has been reported for HCV (Backes et al., 2010).

The reduction of viral proteins, dsRNA, and virus production as a consequence of AnxA2 knockdown could also be related with an impairment of earlier steps during infection, such as virus binding and/or entry. To this regard, it is known that AnxA2 is implicated in the cellular entry of the rabbit vesivirus (RaV), another member of the *Caliciviridae* family (Gonzalez-Reyes et al., 2009). Moreover, AnxA2 can enhance the entry and infectivity of enterovirus 71 (EV71) (Yang et al., 2011), and is involved in the avian leucosis virus-*j* (ALV-J) entry (Mei et al., 2015).

In conclusion, our results demonstrate that AnxA2 has a role during FCV infection. Further studies will be needed to determine the specific role of this host protein in the FCV life cycle.

Funding

This work was supported by Consejo Nacional de Ciencia y Tecnología, grant number 0250696.

Acknowledgments

We thank Rosa M. del Angel and Juan Ludert for helpful suggestions, and critical comments on the manuscript and Salvador Barrera for technical assistance.

Appendix A. Supplementary data

Supplementary material related to this article can be found, in the online version, at doi:https://doi.org/10.1016/j.virusres.2018.12.003.

References

Abente, E.J., Sosnovtsev, S.V., Sandoval-Jaime, C., Parra, G.I., Bok, K., Green, K.Y., 2013. The feline calicivirus leader of the capsid protein is associated with cytopathic effect. J. Virol. 87 (6), 3003–3017.

Alhatlani, B., Vashist, S., Goodfellow, I., 2015. Functions of the 5' and 3' ends of calicivirus genomes. Virus Res. 206, 134–143.

Aukrust, I., Rosenberg, L.A., Ankerud, M.M., Bertelsen, V., Hollas, H., Saraste, J., Grindheim, A.K., Vedeler, A., 2017. Post-translational modifications of Annexin A2 are linked to its association with perinuclear nonpolysomal mRNP complexes. FEBS Open Biol. 7 (2), 160–173.

Babiychuk, E.B., Draeger, A., 2000. Annexins in cell membrane dynamics: Ca2+-regulated association of lipid microdomains. J. Cell Biol. 150 (5), 1113–1123.

Backes, P., Quinkert, D., Reiss, S., Binder, M., Zayas, M., Rescher, U., Gerke, V., Bartenschlager, R., Lohmann, V., 2010. Role of annexin A2 in the production of infectious hepatitis C virus particles. J. Virol. 84 (11), 5775–5789.

Bailey, D., Karakasiliotis, I., Vashist, S., Chung, L.M.W., Rees, J., McFadden, N., Benson, A., Yarovinsky, F., Simmonds, P., Goodfellow, I., 2010. Functional analysis of RNA structures present at the 3' extremity of the murine norovirus genome: the variable polypyrimidine tract plays a role in viral virulence (vol 84, pg 2859-2870). J. Virol. 84 (20) 10943-10943.

Cai, Y., Fukushi, H., Koyasu, S., Kuroda, E., Yamaguchi, T., Hirai, K., 2002. An etiological investigation of domestic cats with conjunctivitis and upper respiratory tract disease in Japan. J. Vet. Med. Sci. 64 (3), 215–219.

Cancio-Lonches, C., Yocupicio-Monroy, M., Sandoval-Jaime, C., Galvan-Mendoza, I., Urena, L., Vashist, S., Goodfellow, I., Salas-Benito, J., Lorena Gutierrez-Escolano, A., 2011. Nucleolin interacts with the feline calicivirus 3' untranslated region and the protease-polymerase NS6 and NS7 proteins, playing a role in virus replication. J. Virol. 85 (16), 8056–8068.

Carter, M.J., 1990. Transcription of feline calicivirus RNA. Arch. Virol. 114 (3-4), 143–152.

Chiang, Y., Rizzino, A., Sibenaller, Z.A., Wold, M.S., Vishwanatha, J.K., 1999. Specific down-regulation of annexin II expression in human cells interferes with cell proliferation. Mol. Cell. Biochem. 199 (1-2), 139–147.

Ellis, T.M., 1981. Jaundice in a Siamese cat with in utero feline calicivirus infection. Aust. Vet. J. 57 (8), 383–385.

Escobar-Herrera, J., Cancio, C., Guzman, G.I., Villegas-Sepulveda, N., Estrada-Garcia, T., Garcia-Lozano, H., Gomez-Santiago, F., Gutierrez-Escolano, A.L., 2006. Construction of an internal RT-PCR standard control for the detection of human caliciviruses in stool. J. Virol. Methods 137 (2), 334–338.

Filipenko, N.R., MacLeod, T.J., Yoon, C.S., Waisman, D.M., 2004. Annexin A2 is a novel RNA-binding protein. J. Biol. Chem. 279 (10), 8723–8731.

Gerke, V., Moss, S.E., 2002. Annexins: from structure to function. Physiol. Rev. 82 (2), 331–371.

Gonzalez-Reyes, S., Garcia-Manso, A., del Barrio, G., Dalton, K.P., Gonzalez-Molleda, L., Arrojo-Fernandez, J., Nicieza, I., Parra, F., 2009. Role of annexin A2 in cellular entry of rabbit vesivirus. J. Gen. Virol. 90 (Pt 11), 2724–2730.

Green, K.Y., Mory, A., Fogg, M.H., Weisberg, A., Belliot, G., Wagner, M., Mitra, T., Ehrenfeld, E., Cameron, C.E., Sosnovtsev, S.V., 2002. Isolation of enzymatically active replication complexes from feline calicivirus-infected cells. J. Virol. 76 (17),

8582–8595.
Grindheim, A.K., Saraste, J., Vedeler, A., 2017. Protein phosphorylation and its role in the regulation of Annexin A2 function. Biochim. Biophys. Acta 1861 (11 Pt A), 2515–2529.
Guo, H., Miao, Q., Zhu, J., Yang, Z., Liu, G., 2018. Isolation and molecular characterization of a virulent systemic feline calicivirus isolated in China. Infect. Genet. Evol. 65, 425–429.
Gutierrez-Escolano, A.L., 2014. Host-cell factors involved in the calicivirus replicative cycle. Future Virol. 9 (2), 147–160.
Gutierrez-Escolano, A.L., Brito, Z.U., del Angel, R.M., Jiang, X., 2000. Interaction of cellular proteins with the 5' end of Norwalk virus genomic RNA. J. Virol. 74 (18), 8558–8562.
Gutierrez-Escolano, A.L., Vazquez-Ochoa, M., Escobar-Herrera, J., Hernandez-Acosta, J., 2003. La, PTB, and PAB proteins bind to the 3' untranslated region of Norwalk virus genomic RNA. Biochem. Biophys. Res. Commun. 311 (3), 759–766.
Harrison, T.M., Sikarskie, J., Kruger, J., Wise, A., Mullaney, T.P., Kiupel, M., Maes, R.K., 2007. Systemic calicivirus epidemic in captive exotic felids. J. Zoo Wildl. Med. 38 (2), 292–299.
Herbert, T.P., Brierley, I., Brown, T.D., 1997. Identification of a protein linked to the genomic and subgenomic mRNAs of feline calicivirus and its role in translation. J. Gen. Virol. 78 (Pt 5), 1033–1040.
Hernandez, B.A., Sandoval-Jaime, C., Sosnovtsev, S.V., Green, K.Y., Gutierrez-Escolano, A.L., 2016. Nucleolin promotes in vitro translation of feline calicivirus genomic RNA. Virology 489, 51–62.
Hollas, H., Aukrust, I., Grimmer, S., Strand, E., Flatmark, T., Vedeler, A., 2006. Annexin A2 recognises a specific region in the 3'-UTR of its cognate messenger RNA. Biochim. Biophys. Acta 1763 (11), 1325–1334.
Karakasiliotis, I., Chaudhry, Y., Roberts, L.O., Goodfellow, I.G., 2006. Feline calicivirus replication: requirement for polypyrimidine tract-binding protein is temperature-dependent. J. Gen. Virol. 87, 3339–3347.
Karakasiliotis, I., Vashist, S., Bailey, D., Abente, E.J., Green, K.Y., Roberts, L.O., Sosnovtsev, S.V., Goodfellow, I.G., 2010. Polypyrimidine tract binding protein functions as a negative regulator of feline calicivirus translation. PLoS One 5 (3), e9562.
Kazami, T., Nie, H., Satoh, M., Kuga, T., Matsushita, K., Kawasaki, N., Tomonaga, T., Nomura, F., 2015. Nuclear accumulation of annexin A2 contributes to chromosomal instability by coilin-mediated centromere damage. Oncogene 34 (32), 4177–4189.
Knowles, J.O., Gaskell, R.M., Gaskell, C.J., Harvey, C.E., Lutz, H., 1989. Prevalence of feline calicivirus, feline leukaemia virus and antibodies to FIV in cats with chronic stomatitis. Vet. Rec. 124 (13), 336–338.
Kwak, H., Park, M.W., Jeong, S., 2011. Annexin A2 binds RNA and reduces the frameshifting efficiency of infectious bronchitis virus. PLoS One 6 (8), e24067.
Li, J.N., Guo, D.W., Huang, L., Yin, M.M., Liu, Q.F., Wang, Y., Yang, C.M., Liu, Y.Y., Zhang, L.J., Tian, Z.J., Cai, X.H., Yu, L.Y., Weng, C.J., 2014a. The interaction between host Annexin A2 and viral Nsp9 is beneficial for replication of porcine reproductive and respiratory syndrome virus. Virus Res. 189, 106–113.
Li, X., Kazan, H., Lipshitz, H.D., Morris, Q.D., 2014b. Finding the target sites of RNA-binding proteins. Wiley Interdiscip. Rev. RNA 5 (1), 111–130.
Liao, K.C., Chuo, V., Ng, W.C., Neo, S.P., Pompon, J., Gunaratne, J., Ooi, E.E., Garcia-Blanco, M.A., 2018. Identification and characterization of host proteins bound to dengue virus 3' UTR reveal an antiviral role for quaking proteins. Rna 24 (6), 803–814.
Ma, Y., Sun, J., Gu, L., Bao, H., Zhao, Y., Shi, L., Yao, W., Tian, G., Wang, X., Chen, H., 2017. Annexin A2 (ANXA2) interacts with nonstructural protein 1 and promotes the replication of highly pathogenic H5N1 avian influenza virus. BMC Microbiol. 17 (1), 191.
Madureira, P.A., Hill, R., Miller, V.A., Giacomantonio, C., Lee, P.W.K., Waisman, D.M., 2011. Annexin A2 is a novel cellular redox regulatory protein involved in Tumorigenesis. Oncotarget 2 (12), 1075–1093.
Mei, M., Ye, J., Qin, A., Wang, L., Hu, X., Qian, K., Shao, H., 2015. Identification of novel viral receptors with cell line expressing viral receptor-binding protein. Sci. Rep. 5, 7935.
Mickleburgh, I., Burtle, B., Hollas, H., Campbell, G., Chrzanowska-Lightowlers, Z., Vedeler, A., Hesketh, J., 2005. Annexin A2 binds to the localization signal in the 3' untranslated region of c-myc mRNA. FEBS J. 272 (2), 413–421.
Morel, E., Gruenberg, J., 2007. The p11/S100A10 light chain of annexin A2 is dispensable for annexin A2 association to endosomes and functions in Endosomal Transport. PLoS One 2 (10).
Moss, S.E., Morgan, R.O., 2004. The annexins. Genome Biol. 5 (4), 219.
Neill, J.D., Reardon, I.M., Heinrikson, R.L., 1991. Nucleotide sequence and expression of the capsid protein gene of feline calicivirus. J. Virol. 65 (10), 5440–5447.
Rentero, C., Blanco-Munoz, P., Meneses-Salas, E., Grewal, T., Enrich, C., 2018. Annexins-coordinators of cholesterol homeostasis in endocytic pathways. Int. J. Mol. Sci. 19 (5).
Rescher, U., Gerke, V., 2004. Annexins–unique membrane binding proteins with diverse functions. J. Cell. Sci. 117 (Pt 13), 2631–2639.
Sarafian, T., Pradel, L.A., Henry, J.P., Aunis, D., Bader, M.F., 1991. The participation of annexin-ii (Calpactin-I) in calcium-evoked exocytosis requires Protein-Kinase-C. J. Cell Biol. 114 (6), 1135–1147.
Saxena, V., Lai, C.K., Chao, T.C., Jeng, K.S., Lai, M.M.C., 2012. Annexin A2 is involved in the formation of hepatitis C virus replication complex on the lipid raft. J. Virol. 86 (8), 4139–4150.
Sheng, C., Liu, X., Jiang, Q., Xu, B., Zhou, C., Wang, Y., Chen, J., Xiao, M., 2015. Annexin A2 is involved in the production of classical swine fever virus infectious particles. J. Gen. Virol. 96 (Pt 5), 1027–1032.
Shwetha, S., Kumar, A., Mullick, R., Vasudevan, D., Mukherjee, N., Das, S., 2015. HuR displaces polypyrimidine tract binding protein to facilitate La binding to the 3' untranslated region and enhances hepatitis C virus replication. J. Virol. 89 (22), 11356–11371.
Simmonds, P., Karakasiliotis, I., Bailey, D., Chaudhry, Y., Evans, D.J., Goodfellow, I.G., 2008. Bioinformatic and functional analysis of RNA secondary structure elements among different genera of human and animal caliciviruses. Nucleic Acids Res. 36 (8), 2530–2546.
Solbak, S.M.O., Abdurakhmanov, E., Vedeler, A., Danielson, U.H., 2017. Characterization of interactions between hepatitis C virus NS5B polymerase, annexin A2 and RNA - effects on NS5B catalysis and allosteric inhibition. Virol. J. 14 (1), 236.
Sosnovtsev, S., Green, K.Y., 1995. RNA transcripts derived from a cloned full-length copy of the feline calicivirus genome do not require VpG for infectivity. Virology 210 (2), 383–390.
Sosnovtsev, S.V., Sosnovtseva, S.A., Green, K.Y., 1998. Cleavage of the feline calicivirus capsid precursor is mediated by a virus-encoded proteinase. J. Virol. 72 (4), 3051–3059.
Sosnovtsev, S.V., Prikhod'ko, E.A., Belliot, G., Cohen, J.I., Green, K.Y., 2003. Feline calicivirus replication induces apoptosis in cultured cells. Virus Res. 94 (1), 1–10.
Stewart, S.E., Ashkenazi, A., Williamson, A., Rubinsztein, D.C., Moreau, K., 2018. Transbilayer phospholipid movement facilitates the translocation of annexin across membranes. J. Cell. Sci. 131 (14).
Thiel, H.J., Konig, M., 1999. Caliciviruses: an overview. Vet. Microbiol. 69 (1-2), 55–62.
Vashist, S., Urena, L., Chaudhry, Y., Goodfellow, I., 2012. Identification of RNA-protein interaction networks involved in the norovirus life cycle. J. Virol. 86 (22), 11977–11990.
Vashist, S., Urena, L., Gonzalez-Hernandez, M.B., Choi, J., de Rougemont, A., Rocha-Pereira, J., Neyts, J., Hwang, S., Wobus, C.E., Goodfellow, I., 2015. Molecular chaperone Hsp90 is a therapeutic target for noroviruses. J. Virol. 89 (12), 6352–6363.
Veyrune, J.L., Campbell, G.P., Wiseman, J., Blanchard, J.M., Hesketh, J.E., 1996. A localisation signal in the 3' untranslated region of c-myc mRNA targets c-myc mRNA and beta-globin reporter sequences to the perinuclear cytoplasm and cytoskeletal-bound polysomes. J. Cell. Sci. 109 (Pt 6), 1185–1194.
Yang, S.L., Chou, Y.T., Wu, C.N., Ho, M.S., 2011. Annexin II binds to capsid protein VP1 of enterovirus 71 and enhances viral infectivity. J. Virol. 85 (22), 11809–11820.
Zhang, C., Xue, C., Li, Y., Kong, Q., Ren, X., Li, X., Shu, D., Bi, Y., Cao, Y., 2010. Profiling of cellular proteins in porcine reproductive and respiratory syndrome virus virions by proteomics analysis. Virol. J. 7, 242.